

RESEARCH ARTICLE

Fixed-time control of teleoperation systems based on adaptive event-triggered communication and force estimators

Xia Liu  and Hui Wen

School of Electrical Engineering and Electronic Information, Xihua University, Chengdu, China

Corresponding author: Xia Liu; Email: xliucd@163.com

Received: 8 May 2024; **Revised:** 12 June 2024; **Accepted:** 17 June 2024

Keywords: teleoperation systems; communication network; adaptive event triggering; force estimators; fixed-time control

Abstract

A fixed-time control strategy based on adaptive event-triggered communication and force estimators is proposed for a class of teleoperation systems with time-varying delays and limited bandwidth. Two force estimators are designed to estimate the operator force and environment force instead of force sensors. With the position, velocity, force estimate signals, and triggering error, an adaptive event-triggered scheme is designed, which automatically adjusts the triggering thresholds to reduce the access frequency of the communication network. With the state information transmitted at the moment of event triggering while considering the time-varying delays, a fixed-time sliding mode controller is designed to achieve the position and force tracking. The stability of the system and the convergence of tracking error within a fixed time are mathematically proved. Experimental results indicate that the control strategy can significantly reduce the information transmission, enhance the bandwidth utilization, and ensure the convergence of tracking error within a fixed time for teleoperation systems.

1. Introduction

Teleoperation systems extend human's capabilities to remote workspaces, such as space exploration, undersea resource exploration, medical rescue, and environment monitoring [1]. In a teleoperation system, the operator manipulates the master robot, sends control commands via the communication network to the slave robot, and enables the slave to track the master's commands in the remote environment. Meanwhile, the slave provides environment force feedback to the master, enhancing the transparency of the teleoperation system [2, 3].

Due to the data exchange between the master and slave in the communication network, time-varying delays (TVDs) are inevitable. For teleoperation systems with TVDs, sliding mode control (SMC) is widely used due to its strong robustness [4]. In ref. [5], a finite-time SMC was proposed for bilateral teleoperation systems with TVDs to ensure the stability and transient response performance of the system. In ref. [6], a terminal SMC was proposed for teleoperation systems with TVDs to stabilize the system and enable the position error to converge in finite time. In ref. [7], for teleoperation systems with TVDs and dynamic uncertainty, a finite-time SMC was proposed to ensure system stability and finite-time convergence. However, in refs. [5–7] the convergence time depends on the initial values of the system states. To solve this problem, in ref. [8] an adaptive fixed-time SMC was designed for teleoperation systems with TVDs and parameter uncertainty to achieve stabilization and trajectory tracking of the system. In ref. [9], an integral SMC was proposed for teleoperation systems with TVDs and external disturbance, ensuring the system stability and synchronization error convergence within a fixed time. In ref. [10], for teleoperation systems with TVDs and uncertainty, a fixed-time SMC was designed to

enhance the tracking performance while ensuring the system stability. Although in refs. [8–10] fixed-time convergence of the position tracking can be achieved, the force tracking is not considered and thus the transparency of the teleoperation systems cannot be guaranteed.

Good transparency improves the capacity of operator to execute complex tasks, requiring accurate perception of the interaction force between the slave and the remote environment. Typically, these forces are measured by force sensors, which may be limited by costs and noise [11–13]. To circumvent force sensors, in ref. [14], a PD controller based on force estimator (FE) was designed for teleoperation systems with constant time delays to achieve stable position and force tracking. In ref. [15], an enhanced FE and a passive control strategy were designed to predict the operator force and environment force, ensuring precise position and force tracking of teleoperation systems with constant time delays. In ref. [16], an observer-based control strategy was developed for teleoperation systems with constant time delays to ensure the position and force tracking. In ref. [17], a sliding mode force observer was designed to estimate the operator force and environment force within a fixed time, and a P-like controller was designed to achieve stable position and force tracking of teleoperation systems with TVDs. In ref. [18], a dynamic gain force observer was developed for teleoperation systems with TVDs, which employed adaptive laws and wave variables to obtain satisfactory control performance. Although in refs. [14–18] system transparency is enhanced through force estimator instead of force sensors, fixed-time convergence of tracking error cannot be ensured. Moreover, it is implicitly assured in refs. [14–18] that continuous data transmission is maintained between the master and slave, which is prone to network congestion and degrades the control performance.

In fact, continuous data transmission is unavailability to the communication network in teleoperation systems as the network bandwidth is always limited. Therefore, network congestion inevitably arises, which will degrade the control performance or even making the system unstable. Event-triggered control strategy serves as an effective method to relieve the system from relying on the communication network resources, ensuring system performance while enhancing resource utilization [19]. During event-triggered communication, the transmission of each state depends on its corresponding triggering condition. If the triggering condition is satisfied, the current state information is transmitted. Otherwise, the state information at the last triggering moment is retained. In ref. [20], for teleoperation systems under constant time delays, an event-triggered scheme was constructed by scattering transformation and an adaptive controller was designed to ensure the system stability and position tracking. In ref. [21], for teleoperation systems with constant time delays, an event-triggered scheme was proposed based on joint velocities, and a P-like controller was designed to ensure the system stability and position tracking. In ref. [22], an event-triggered P-like control was investigated for teleoperation systems with TVDs to achieve system stability and position synchronization. In ref. [23], an event-triggered coordination control for teleoperation systems with constant time delays was introduced to ensure the system stability and position tracking, where the event-triggered scheme was constructed based on auxiliary variables associated with position and velocity. In ref. [24], an event-triggered scheme based on norm of sliding mode was designed to enhance the sensitivity of the controller and save the communication network resources in teleoperation systems. In ref. [25], an event-triggered backstepping control for teleoperation systems with constant time delays was proposed, which could achieve system stability within a fixed time and avoid unnecessary resource consumption. In ref. [26], an event-triggered prescribed-time control based on exponential Lyapunov functions was presented for teleoperation systems with multiple constraints and TVDs. However, the triggering thresholds in refs. [20–26] are constant and cannot be adjusted according to the system states, which may waste communication resources and degrade control performance.

Therefore, this paper proposes a fixed-time control strategy for teleoperation systems based on adaptive event-triggered communication and FEs. This strategy flexibly and effectively reduces redundant data transmission and achieves fixed-time convergence of tracking error in teleoperation systems with TVDs. The main contributions of this paper are:

- Two FEs are designed to indirectly acquire the operator force and environment force without force sensors.
- An adaptive event-triggered scheme (AETS) is designed which can automatically adjust the triggering thresholds based on the system states. Compared to the event-triggered scheme with fixed triggering thresholds, the designed AETS can further reduce unnecessary data transmission and conserve network resources.
- A fixed-time SMC is developed by utilizing the FEs and event-triggered states. Compared to the conventional SMC, the fixed-time SMC can ensure the convergence of tracking error within a fixed time under TVDs. Meanwhile, it can guarantee the system stability and enhance the position and force tracking performance.

2. Dynamical model of teleoperation systems

The dynamic model of a teleoperation system with n -DOF master and slave can be described as [7]

$$\begin{aligned} M_m(q_m)\ddot{q}_m + C_m(q_m, \dot{q}_m)\dot{q}_m + g_m(q_m) &= \tau_m + F_h \\ M_s(q_s)\ddot{q}_s + C_s(q_s, \dot{q}_s)\dot{q}_s + g_s(q_s) &= \tau_s + F_e \end{aligned} \tag{1}$$

where the subscript $i = \{m, s\}$ represents the master and slave, respectively. $q_i \in R^{n \times 1}$ represents the joint position, $\dot{q}_i \in R^{n \times 1}$ represents the velocity, $\ddot{q}_i \in R^{n \times 1}$ represents the acceleration. $M_i(q_i) \in R^{n \times n}$ represents the inertia matrix, $C_i(q_i, \dot{q}_i) \in R^{n \times n}$ represents the Coriolis/centrifugal matrix, $g_i(q_i) \in R^{n \times 1}$ represents the gravitational force, $\tau_i \in R^{n \times 1}$ is the control input. $F_h \in R^{n \times 1}$ is the operator force and $F_e \in R^{n \times 1}$ is the environment force.

The dynamic model (1) has the following properties [27–30]:

Property 1: The inertia matrix $M_i(q_i(t))$ is symmetric positive definite and there exist positive constants $\underline{\lambda}_i$ and $\bar{\lambda}_i$ such that $0 < \underline{\lambda}_i I \leq M_i(q_i) \leq \bar{\lambda}_i I$, where $I \in R^{n \times n}$ is the identity matrix.

Property 2: The matrix $\dot{M}_i(q_i) - 2C_i(q_i, \dot{q}_i)$ is skew-symmetric, that is, $x^T(\dot{M}_i(q_i) - 2C_i(q_i, \dot{q}_i))x = 0$ holds for any vector $x \in R^{n \times 1}$.

Property 3: For vectors $p_1, p_2 \in R^{n \times 1}$, there always exists a positive constant \tilde{h}_i such that the Coriolis/centrifugal matrix is bounded, that is, $\|C_i(q_i, p_1)p_2\| \leq \tilde{h}_i \|p_1\| \|p_2\|$.

Property 4: When \dot{q}_i and \ddot{q}_i are bounded, $\dot{C}_i(q_i, \dot{q}_i)$ is also bounded.

3. Design of the control strategy

The proposed fixed-time control strategy based on adaptive event-triggered communication and FEs is shown in Figure 1. Firstly, the FEs are used to acquire the estimate of the operator force w_h and environment force w_e . Further, the transmission of the position, velocity, and the estimate of the environment force are regulated by the AETS. Finally, the fixed-time SMC ensures that the tracking error of the teleoperation systems under TVDs $T_1(t)$ and $T_2(t)$ converges within a fixed time.

3.1. FEs

Two FEs are designed to acquire the operator force and environment force instead of directly using force sensors.

The FE for the master is designed as

$$\begin{aligned} w_h(t) &= \mathcal{Z}_m(t) + y_m(\dot{q}_m) \\ \dot{\mathcal{Z}}_m(t) &= -\ell_h \mathcal{Z}_m(t) + \ell_h (C_m \dot{q}_m + g_m - \tau_m - y_m(\dot{q}_m)) - \mathcal{P}_m \dot{q}_m \end{aligned} \tag{2}$$

where $w_h(t) = \hat{F}_h$ is the estimate of the operator force F_h , \mathcal{P}_m is a positive definite gain matrix and $\ell_h = \chi_m M_m^{-1}(q_m)$. Let

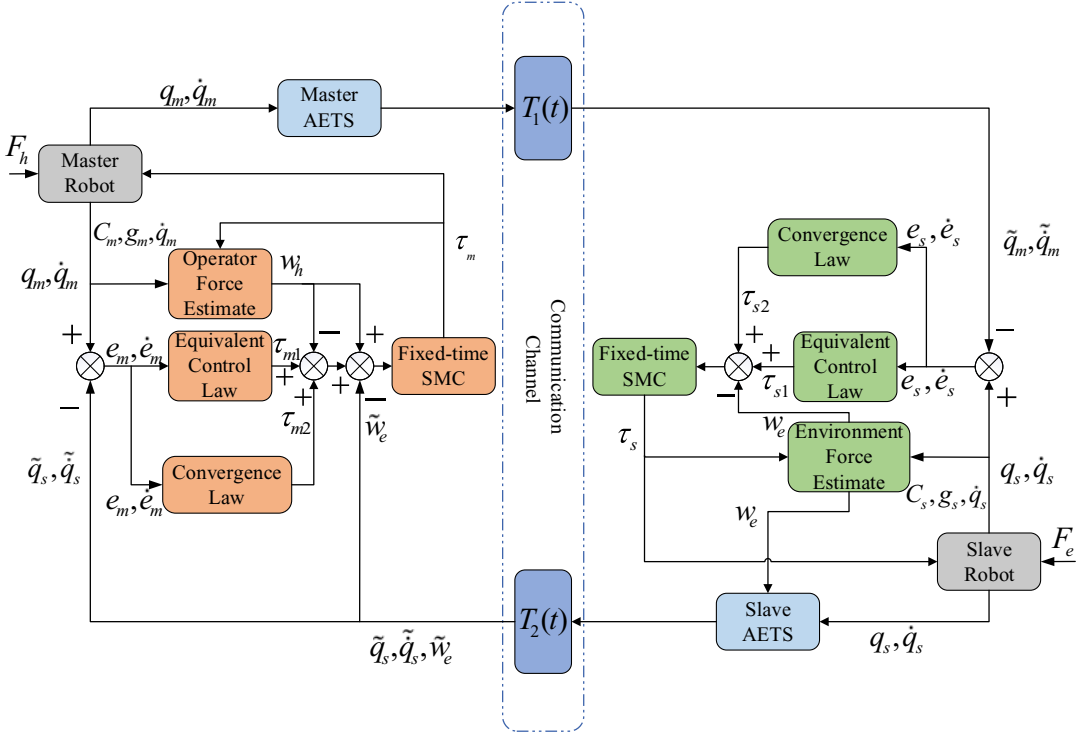


Figure 1. Block diagram of fixed-time control strategy based on adaptive event-triggered communication and FEs.

$$\dot{y}_m(\dot{q}_m) = \ell_h M_m(q_m) \ddot{q}_m \tag{3}$$

Substituting ℓ_h into (3) and integrating its both sides yield

$$y_m(\dot{q}_m) = \chi_m \dot{q}_m \tag{4}$$

where $\chi_m > 0$ is a constant. Define the estimate error of the operator force as $\bar{F}_h = F_h - w_h$. Then from (2) to (4), it yields

$$\begin{aligned} \dot{\bar{F}}_h &= \dot{F}_h - \dot{w}_h \\ &= \dot{F}_h + \ell_h(w_h - y_m(\dot{q}_m)) - \ell_h(M_m(q_m)\ddot{q}_m + C_m\dot{q}_m + g_m - \tau_m) + \mathcal{P}_m\dot{q}_m + \ell_h y_m(\dot{q}_m) \\ &= \dot{F}_h - \ell_h \bar{F}_h + \mathcal{P}_m\dot{q}_m \end{aligned} \tag{5}$$

Similarly, the FE for the slave is designed as

$$\begin{aligned} w_e(t) &= \mathcal{Z}_s(t) + y_s(\dot{q}_s) \\ \dot{\mathcal{Z}}_s(t) &= -\ell_e \mathcal{Z}_s(t) + \ell_e(C_s\dot{q}_s + g_s - \tau_s - y_s(\dot{q}_s)) - \mathcal{P}_s\dot{q}_s - \mathcal{Q}q_s \end{aligned} \tag{6}$$

where $w_e(t) = \hat{F}_e$ is the estimate of the environment force F_e . Besides, $\mathcal{P}_s, \mathcal{Q}$ are positive definite gain matrices and $\ell_e = \chi_s M_s^{-1}(q_s)$. Let

$$\dot{y}_s(\dot{q}_s) = \ell_e M_s(q_s) \ddot{q}_s \tag{7}$$

Substituting ℓ_e into (7) and integrating its both sides yield

$$y_s(\dot{q}_s) = \chi_s \dot{q}_s \tag{8}$$

where $\chi_s > 0$ is a constant. Define the estimate error of the environment force as $\bar{F}_e = F_e - w_e$. Then from (6) to (8), it yields

$$\begin{aligned} \dot{\bar{F}}_e &= \dot{F}_e - \dot{w}_e \\ &= \dot{F}_e + \ell_e(w_e - y_s(\dot{q}_s)) - \ell_e(M_s(q_s)\ddot{q}_s + C_s\dot{q}_s + g_s - \tau_s) + \mathcal{P}_s\dot{q}_s + \mathcal{Q}q_s + \ell_e y_s(\dot{q}_s) \\ &= \dot{F}_e - \ell_e \bar{F}_e + \mathcal{P}_s\dot{q}_s + \mathcal{Q}q_s \end{aligned} \tag{9}$$

In practice, the operator force and the environment force are usually bounded, that is, $\|F_h\| < \mathcal{F}_h, \|F_e\| < \mathcal{F}_e$ [17]. However, since the bounds \mathcal{F}_h and \mathcal{F}_e are usually unknown, the following adaptive laws are designed to estimate them

$$\begin{aligned} \dot{\hat{\mathcal{F}}}_h &= \bar{F}_h^T (\dot{\bar{F}}_h + \ell_h \bar{F}_h) \\ \dot{\hat{\mathcal{F}}}_e &= \bar{F}_e^T (\dot{\bar{F}}_e + \ell_e \bar{F}_e) \end{aligned} \tag{10}$$

Theorem 1. For the teleoperation system (1) under TVDs, using the FEs (2), (6) and the adaptive laws (10), the estimate errors of the operator force and environment force asymptotically converge to zero, that is, $\lim_{t \rightarrow \infty} \bar{F}_e \rightarrow 0$ and $\lim_{t \rightarrow \infty} \bar{F}_h \rightarrow 0$.

Proof: Define a Lyapunov function as

$$V_1 = \frac{1}{2} \bar{F}_h^T \bar{F}_h + \frac{1}{2} \bar{F}_e^T \bar{F}_e + \frac{1}{2} (\mathcal{F}_h - \hat{\mathcal{F}}_h)^2 + \frac{1}{2} (\mathcal{F}_e - \hat{\mathcal{F}}_e)^2 \tag{11}$$

Differentiating (11) and substituting (5) and (9) into it, we have

$$\begin{aligned} \dot{V}_1 &= \bar{F}_h^T \dot{\bar{F}}_h + \bar{F}_e^T \dot{\bar{F}}_e - \dot{\hat{\mathcal{F}}}_h - \dot{\hat{\mathcal{F}}}_e \\ &= \bar{F}_h^T (\dot{F}_h - \ell_h \bar{F}_h + \mathcal{P}_m \dot{q}_m) + \bar{F}_e^T (\dot{F}_e - \ell_e \bar{F}_e + \mathcal{P}_s \dot{q}_s + \mathcal{Q}q_s) - \dot{\hat{\mathcal{F}}}_h - \dot{\hat{\mathcal{F}}}_e \end{aligned} \tag{12}$$

Substituting the adaptive laws (10) into (12) yields

$$\dot{V}_1 \leq -\ell_h \bar{F}_h^T \bar{F}_h - \ell_e \bar{F}_e^T \bar{F}_e \tag{13}$$

Since $\ell_h = \chi_m M_m^{-1}(q_m), \ell_e = \chi_s M_s^{-1}(q_s), \chi_m$ and χ_s are positive constants, and both $M_m^{-1}(q_m)$ and $M_s^{-1}(q_s)$ are positive definite matrices, it follows that $\dot{V}_1 \leq 0$. Consequently, \bar{F}_h and \bar{F}_e are bounded. Also, $\dot{V}_1 = 0$ holds if and only if $\bar{F}_h = 0$ and $\bar{F}_e = 0$. Hence, the estimate errors of the operator force \bar{F}_h and environment force \bar{F}_e asymptotically converge to zero, that is, $\lim_{t \rightarrow \infty} \bar{F}_e \rightarrow 0$ and $\lim_{t \rightarrow \infty} \bar{F}_h \rightarrow 0$.

3.2. AETS

To save limited network resources, the AETS is designed as Figure 2. The adaptive triggering thresholds and triggering errors constitute the triggering conditions. Then, an event detector (ED) evaluates these conditions. Once the triggering conditions are satisfied, the state information is allowed to transit through the communication network. Simultaneously, the zero-order hold (ZOH) preserves the state information that meets the triggering conditions until the next triggering moment occurs.

Define the triggered position error and triggered velocity error for the master as

$$\begin{aligned} e_m^q &= q_m - \hat{q}_m \\ e_m^v &= \dot{q}_m - \hat{\dot{q}}_m \end{aligned} \tag{14}$$

where $\hat{q}_m = q_m(t_1^{mq})$ and $\hat{\dot{q}}_m = \dot{q}_m(t_1^{mv})$ are the triggered position and triggered velocity transmitted at the current triggering moment. Therefore, the adaptive event-triggering conditions are designed as

$$\begin{aligned} (e_m^q)^T \Xi_m e_m^q &> \delta_1 \dot{q}_m^T \Xi_m \dot{q}_m \\ (e_m^v)^T \Xi_m e_m^v &> \delta_2 \dot{q}_m^T \Xi_m \dot{q}_m \end{aligned} \tag{15}$$

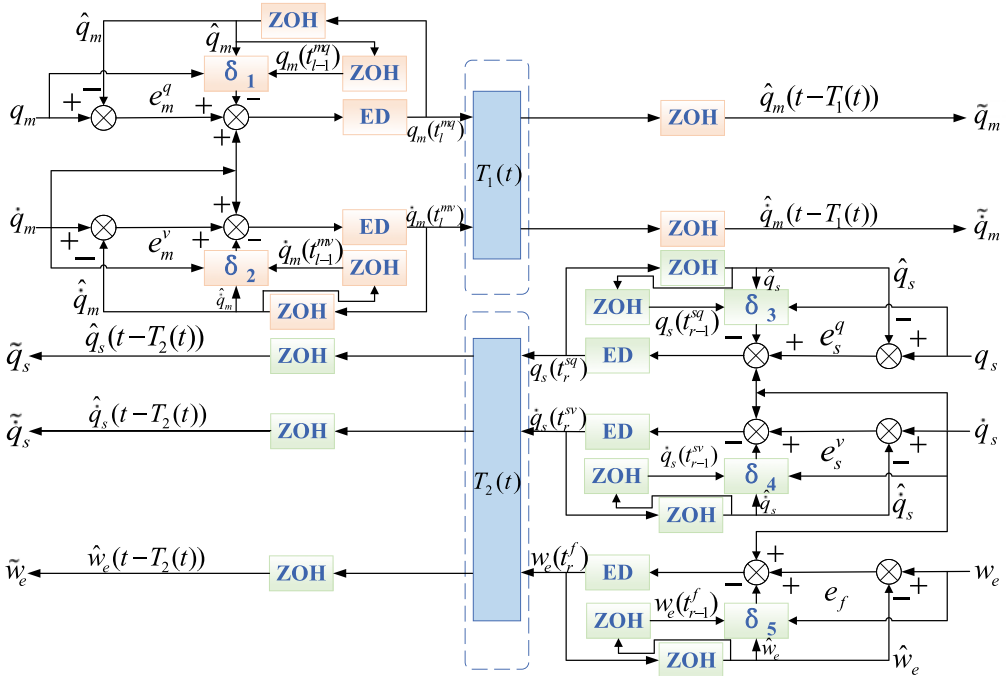


Figure 2. Block diagram of AETS.

where Ξ_m is the weighted matrix of the triggering conditions, and δ_1, δ_2 are adaptive triggering thresholds for the master designed as

$$\begin{aligned} \delta_1 &= \max(\delta_{1\min}, \min(\delta_{1\max}, \mathcal{E}_1), \mathcal{J}_1) \\ \delta_2 &= \max(\delta_{2\min}, \min(\delta_{2\max}, \mathcal{E}_2), \mathcal{J}_2) \end{aligned} \tag{16}$$

where $\delta_{1\min}$ and $\delta_{1\max}$, $\delta_{2\min}$ and $\delta_{2\max}$ represent the minimum and maximum values of the position triggering threshold, velocity triggering threshold for the master, respectively. Also,

$$\begin{aligned} \mathcal{E}_1 &= a * \tanh\left(\frac{\|q_m - \hat{q}_m\|}{\|q_m + \hat{q}_m\|}\right) * \delta_{1ed} \\ \mathcal{E}_2 &= a * \tanh\left(\frac{\|\dot{q}_m - \hat{\dot{q}}_m\|}{\|\dot{q}_m + \hat{\dot{q}}_m\|}\right) * \delta_{2ed} \end{aligned} \tag{17}$$

In (17), $a > 0$, δ_{1ed} and δ_{2ed} represent the adaptive triggering thresholds of the position and velocity for the master at the last triggering moment, respectively. When the triggering conditions (15) are satisfied, the values of δ_{1ed} and δ_{2ed} are updated to the current triggering thresholds δ_1 and δ_2 . In addition, the initial values of δ_{1ed} and δ_{2ed} are $\delta_{1\max}$ and $\delta_{2\max}$. Besides, \mathcal{J}_1 and \mathcal{J}_2 are

$$\begin{aligned} \mathcal{J}_1 &= e^{b*} \|\| \hat{q}_m \| - \| q_m(t_{l-1}^{mq}) \| \| \\ \mathcal{J}_2 &= e^{b*} \|\| \hat{\dot{q}}_m \| - \| \dot{q}_m(t_{l-1}^{mv}) \| \| \end{aligned} \tag{18}$$

where $b < 0$, and $q_m(t_{l-1}^{mq}), \dot{q}_m(t_{l-1}^{mv})$ represent the triggered position and triggered velocity transmitted at the last triggering moment. Notice that when $b > 0$, the values of \mathcal{J}_1 or \mathcal{J}_2 may easily exceed $\delta_{1\max}$ or $\delta_{2\max}$. Therefore, to ensure $\mathcal{J}_1 < \delta_{1\max}$ and $\mathcal{J}_2 < \delta_{2\max}$, b must be less than 0.

Now, define the triggered position error, triggered velocity error, and triggered estimate error of the environment force for the slave as

$$\begin{aligned} e_s^q &= q_s - \hat{q}_s \\ e_s^v &= \dot{q}_s - \hat{\dot{q}}_s \\ e_f &= w_e - \hat{w}_e \end{aligned} \tag{19}$$

where $\hat{q}_s = q_s(t_r^{sq})$, $\hat{\dot{q}}_s = \dot{q}_s(t_r^{sv})$ and $\hat{w}_e = w_e(t_r^f)$. Thus, the adaptive event-triggering conditions for the slave are designed as

$$\begin{aligned} (e_s^q)^T \Xi_s e_s^q &> \delta_3 \dot{q}_s^T \Xi_s \dot{q}_s \\ (e_s^v)^T \Xi_s e_s^v &> \delta_4 \dot{q}_s^T \Xi_s \dot{q}_s \\ (e_f)^T \Xi_s e_f &> \delta_5 \dot{q}_s^T \Xi_s \dot{q}_s \end{aligned} \tag{20}$$

where Ξ_s is the weighted matrix of the triggering conditions, and δ_3 , δ_4 and δ_5 are the adaptive triggering thresholds for the slave designed as

$$\begin{aligned} \delta_3 &= \max(\delta_{3\min}, \min(\delta_{3\max}, \mathcal{E}_3), \mathcal{J}_3) \\ \delta_4 &= \max(\delta_{4\min}, \min(\delta_{4\max}, \mathcal{E}_4), \mathcal{J}_4) \\ \delta_5 &= \max(\delta_{5\min}, \min(\delta_{5\max}, \mathcal{E}_5), \mathcal{J}_5) \end{aligned} \tag{21}$$

where $\delta_{3\min}$ and $\delta_{3\max}$, $\delta_{4\min}$ and $\delta_{4\max}$, $\delta_{5\min}$ and $\delta_{5\max}$ represent the minimum and maximum values of the position triggering threshold, velocity triggering threshold, and the estimate of the environment force triggering threshold for the slave, respectively. Additionally,

$$\begin{aligned} \mathcal{E}_3 &= a * \tanh\left(\frac{\|q_s - \hat{q}_s\|}{\|q_s + \hat{q}_s\|}\right) * \delta_{3ed} \\ \mathcal{E}_4 &= a * \tanh\left(\frac{\|\dot{q}_s - \hat{\dot{q}}_s\|}{\|\dot{q}_s + \hat{\dot{q}}_s\|}\right) * \delta_{4ed} \\ \mathcal{E}_5 &= a * \tanh\left(\frac{\|w_e - \hat{w}_e\|}{\|w_e + \hat{w}_e\|}\right) * \delta_{5ed} \end{aligned} \tag{22}$$

In (22), $a > 0$ is a constant, δ_{3ed} , δ_{4ed} , and δ_{5ed} represent the adaptive triggering thresholds of the position, velocity, and the estimate of the environment force for the slave at the last triggering moment, respectively. When the triggering conditions (20) are satisfied, the values of δ_{3ed} , δ_{4ed} , and δ_{5ed} are updated to the current triggering thresholds δ_3 , δ_4 , and δ_5 . In addition, the initial values of δ_{3ed} , δ_{4ed} , and δ_{5ed} are set to $\delta_{3\max}$, $\delta_{4\max}$ and $\delta_{5\max}$. Besides, \mathcal{J}_3 , \mathcal{J}_4 , and \mathcal{J}_5 in (21) are

$$\begin{aligned} \mathcal{J}_3 &= e^{b*} \|\hat{q}_s\| - \|q_s(t_{r-1}^{sq})\| \\ \mathcal{J}_4 &= e^{b*} \|\hat{\dot{q}}_s\| - \|\dot{q}_s(t_{r-1}^{sv})\| \\ \mathcal{J}_5 &= e^{b*} \|\hat{w}_e\| - \|w_e(t_{r-1}^f)\| \end{aligned} \tag{23}$$

In (23), $b < 0$, and $q_s(t_{r-1}^{sq})$, $\dot{q}_s(t_{r-1}^{sv})$ and $w_e(t_{r-1}^f)$ represent the triggered position, triggered velocity and triggered estimate of the environment force transmitted at the last triggering moment, respectively. From (18) and (23) one can see that the adaptive triggering thresholds include the current triggered values as well as the last triggered values of the position, velocity for the master and slave, and the estimate of the environment force.

Now, the AETS can be designed as

$$\begin{aligned}
 t_{l+1}^{mq} &= \inf \left\{ t > t_l^{mq} \mid (e_m^q)^T \Xi_m e_m^q > \delta_1 \dot{q}_m^T \Xi_m \dot{q}_m \right\} \\
 t_{l+1}^{mv} &= \inf \left\{ t > t_l^{mv} \mid (e_m^v)^T \Xi_m e_m^v > \delta_2 \dot{q}_m^T \Xi_m \dot{q}_m \right\} \\
 t_{r+1}^{sq} &= \inf \left\{ t > t_r^{sq} \mid (e_s^q)^T \Xi_s e_s^q > \delta_3 \dot{q}_s^T \Xi_s \dot{q}_s \right\} \\
 t_{r+1}^{sv} &= \inf \left\{ t > t_r^{sv} \mid (e_s^v)^T \Xi_s e_s^v > \delta_4 \dot{q}_s^T \Xi_s \dot{q}_s \right\} \\
 t_{r+1}^f &= \inf \left\{ t > t_r^f \mid (e_f)^T \Xi_s e_f > \delta_5 \dot{q}_s^T \Xi_s \dot{q}_s \right\}
 \end{aligned} \tag{24}$$

where the time series $t_l^{mq}, t_l^{mv}, t_r^{sq}, t_r^{sv}$ and t_r^f denote the current triggering moments of the position for the master, velocity for the master, position for the slave, velocity for the slave, and the estimate of the environment force, respectively. $t_{l+1}^{mq}, t_{l+1}^{mv}, t_{r+1}^{sq}, t_{r+1}^{sv}$, and t_{r+1}^f denote the next triggering moments of $t_l^{mq}, t_l^{mv}, t_r^{sq}, t_r^{sv}$ and t_r^f , where $l \in \mathbb{N}, r \in \mathbb{N}$ and \mathbb{N} denotes the set of natural numbers. As the triggering thresholds are associated with the current and last values of the states, when the triggered errors increase, the event-triggering thresholds will appropriately decrease to increase the data transmission frequency. Conversely, the event-triggering thresholds increase to reduce the data transmission frequency. That is, the triggering thresholds can be dynamically adjusted based on the adaptive triggering thresholds designed in (16) and (21).

Remark 1. In the AETS (24), the next triggering always satisfies the triggering condition and it occurs strictly after the current triggering moment. This prevents the occurrence of zero intervals between two triggering moments, thereby avoiding the Zeno phenomenon.

3.3. Fixed-time SMC

Based on the FEs and AETS presented in Sections 3.1 and 3.2, fixed-time SMC for master and slave will be designed to ensure the convergence of tracking error under TVDs.

Define the position tracking error as

$$\begin{aligned}
 e_m(t) &= q_m(t) - \tilde{q}_s(t) \\
 e_s(t) &= q_s(t) - \tilde{q}_m(t)
 \end{aligned} \tag{25}$$

where $\tilde{q}_m = \hat{q}_m(t - T_1(t))$ and $\tilde{q}_s = \hat{q}_s(t - T_2(t))$ are the triggered positions for the master and slave at the current triggering moment affected by TVDs. Differentiating (25) with respect to time yields

$$\begin{aligned}
 \dot{e}_m(t) &= \dot{q}_m(t) - \dot{\hat{q}}_s(t - T_2(t))(1 - \dot{T}_2(t)) \\
 \dot{e}_s(t) &= \dot{q}_s(t) - \dot{\hat{q}}_m(t - T_1(t))(1 - \dot{T}_1(t)) \\
 \ddot{e}_m(t) &= \ddot{q}_m(t) - \ddot{\hat{q}}_s(t - T_2(t))(1 - \dot{T}_2(t))^2 + \dot{\hat{q}}_s(t - T_2(t))\ddot{T}_2(t) \\
 \ddot{e}_s(t) &= \ddot{q}_s(t) - \ddot{\hat{q}}_m(t - T_1(t))(1 - \dot{T}_1(t))^2 + \dot{\hat{q}}_m(t - T_1(t))\ddot{T}_1(t)
 \end{aligned} \tag{26}$$

According to (25) and (26), the sliding mold surface is designed as

$$\begin{aligned}
 s_m &= \dot{e}_m + k_{m1} \text{sig}(e_m)^{\varphi_{m1}} + k_{m2} \text{sig}(e_m)^{\varphi_{m2}} \\
 s_s &= \dot{e}_s + k_{s1} \text{sig}(e_s)^{\varphi_{s1}} + k_{s2} \text{sig}(e_s)^{\varphi_{s2}}
 \end{aligned} \tag{27}$$

where $k_{m1} > 0, k_{m2} > 0, k_{s1} > 0, k_{s2} > 0$ are constant gains. In addition, $0 < \varphi_{m1} < 1, \varphi_{m2} > 1, 0 < \varphi_{s1} < 1, \varphi_{s2} > 1$, and $sig(\cdot)^{\nu} = |\cdot|^{\nu}sgn(\cdot)$ where $sgn(\cdot)$ is sign function.

Differentiating (27) leads to

$$\begin{aligned} \dot{s}_m &= \ddot{e}_m + k_{m1}\varphi_{m1}diag(|e_m|^{\varphi_{m1}-1})\dot{e}_m + k_{m2}\varphi_{m2}diag(|e_m|^{\varphi_{m2}-1})\dot{e}_m \\ \dot{s}_s &= \ddot{e}_s + k_{s1}\varphi_{s1}diag(|e_s|^{\varphi_{s1}-1})\dot{e}_s + k_{s2}\varphi_{s2}diag(|e_s|^{\varphi_{s2}-1})\dot{e}_s \end{aligned} \tag{28}$$

Therefore, the fixed-time SMC can be designed as

$$\begin{aligned} \tau_m &= \tau_{m1} + \tau_{m2} \\ \tau_s &= \tau_{s1} + \tau_{s2} \end{aligned} \tag{29}$$

where

$$\begin{aligned} \tau_{m1} &= M_m \left(\ddot{\hat{q}}_s(t - T_2(t))(1 - \dot{T}_2(t))^2 - \dot{\hat{q}}_s(t - T_2(t))\ddot{T}_2(t) - k_{m1}\varphi_{m1}diag(|e_m|^{\varphi_{m1}-1})\dot{e}_m \right. \\ &\quad \left. - k_{m2}\varphi_{m2}diag(|e_m|^{\varphi_{m2}-1})\dot{e}_m \right) + C_m(\dot{q}_m - s_m) + g_m - w_h - \wp|w_h - \tilde{w}_e| \\ \tau_{s1} &= M_s \left(\ddot{\hat{q}}_m(t - T_1(t))(1 - \dot{T}_1(t))^2 - \dot{\hat{q}}_m(t - T_1(t))\ddot{T}_1(t) - k_{s1}\varphi_{s1}diag(|e_s|^{\varphi_{s1}-1})\dot{e}_s \right. \\ &\quad \left. - k_{s2}\varphi_{s2}diag(|e_s|^{\varphi_{s2}-1})\dot{e}_s \right) + C_s(\dot{q}_s - s_s) + g_s - w_e \end{aligned} \tag{30}$$

$$\begin{aligned} \tau_{m2} &= -k_{m3}M_msgn(s_m) - k_{m4}M_msig(s_m)^{\sigma_{m1}} - k_{m5}M_msig(s_m)^{\sigma_{m2}} \\ \tau_{s2} &= -k_{s3}M_ssgn(s_s) - k_{s4}M_ssig(s_s)^{\sigma_{s1}} - k_{s5}M_ssig(s_s)^{\sigma_{s2}} \end{aligned} \tag{31}$$

where \wp is a positive definite matrix, $\tilde{w}_e = \hat{w}_e(t - T_2(t)), k_{m3} > 0, k_{m4} > 0, k_{m5} > 0, k_{s3} > 0, k_{s4} > 0$, and $k_{s5} > 0$ are constant gains. Besides, $0 < \sigma_{m1} < 1, \sigma_{m2} > 1, 0 < \sigma_{s1} < 1, \sigma_{s2} > 1$. Eq. (30) is the equivalent control law for the master and slave, while (31) is the double-power convergence law. Compared to the convergence law in the traditional SMC, the double-power convergence law allows the system to have faster convergence.

Substituting (29)-(31) into (1), the closed-loop system is obtained as

$$\begin{aligned} &M_m(q_m)\ddot{q}_m + C_m(q_m, \dot{q}_m)\dot{q}_m + g_m(q_m) \\ &= M_m \left(\ddot{\hat{q}}_s(t - T_2(t))(1 - \dot{T}_2(t))^2 - \dot{\hat{q}}_s(t - T_2(t))\ddot{T}_2(t) - k_{m1}\varphi_{m1}diag(|e_m|^{\varphi_{m1}-1})\dot{e}_m \right. \\ &\quad \left. - k_{m2}\varphi_{m2}diag(|e_m|^{\varphi_{m2}-1})\dot{e}_m \right) + C_m(\dot{q}_m - s_m) + g_m + F_h - w_h - \wp|w_h - \tilde{w}_e| \\ &\quad - k_{m3}M_msgn(s_m) - k_{m4}M_msig(s_m)^{\sigma_{m1}} - k_{m5}M_msig(s_m)^{\sigma_{m2}} \\ &M_s(q_s)\ddot{q}_s + C_s(q_s, \dot{q}_s)\dot{q}_s + g_s(q_s) \\ &= M_s \left(\ddot{\hat{q}}_m(t - T_1(t))(1 - \dot{T}_1(t))^2 - \dot{\hat{q}}_m(t - T_1(t))\ddot{T}_1(t) - k_{s1}\varphi_{s1}diag(|e_s|^{\varphi_{s1}-1})\dot{e}_s \right. \\ &\quad \left. - k_{s2}\varphi_{s2}diag(|e_s|^{\varphi_{s2}-1})\dot{e}_s \right) + C_s(\dot{q}_s - s_s) + g_s + F_e - w_e - k_{s3}M_ssgn(s_s) \\ &\quad - k_{s4}M_ssig(s_s)^{\sigma_{s1}} - k_{s5}M_ssig(s_s)^{\sigma_{s2}} \end{aligned} \tag{32}$$

Lemma 1 [31]: For a nonlinear system $\dot{x} = f(x, t), x(0) = x_0$, if there exists a continuous positive definite Lyapunov function $V(x): R^{n \times 1} \rightarrow R^+$ satisfying

$$\dot{V}(x) \leq -\mathfrak{S}_1 V(x)^a - \mathfrak{S}_2 V(x)^b \tag{33}$$

where $x \in R^{n \times 1}, \mathfrak{S}_1 > 0, \mathfrak{S}_2 > 0$ and $0 < a < 1 < b$. Then, the nonlinear system is globally fixed-time stable with the convergence time bounded by T_{st} as

$$T_{st} \leq \frac{1}{\mathfrak{S}_1} \frac{1}{(1-a)} + \frac{1}{\mathfrak{S}_2} \frac{1}{(b-1)} \tag{34}$$

Theorem 2. For the teleoperation system (1), using the FEs (2), (6), the AETS (24), along with the fixed-time SMC (29) to (31), the system stability within a fixed time T_{sup} is ensured. Moreover, the upper bound of the convergence time for the position tracking error is $T_{sup} = T_{rt} + T_{st} = \frac{1}{k_4} \frac{1}{(1-\sigma_1)} + \frac{1}{k_5} \frac{1}{(\sigma_2-1)} + \frac{1}{k_1} \frac{1}{(1-\varphi_1)} + \frac{1}{k_2} \frac{1}{(\varphi_2-1)}$. Furthermore, the force tracking error also converges to zero. that is, $\lim_{t \rightarrow \infty} (|w_h - \tilde{w}_e|) \rightarrow 0$.

Proof. Define a Lyapunov function as

$$V_2 = \frac{1}{2} s_m^T M_m s_m + \frac{1}{2} s_s^T M_s s_s \tag{35}$$

Differentiating (35), using property 2 and substituting (28) into (35) yield

$$\begin{aligned} \dot{V}_2 = & s_m^T M_m (\ddot{e}_m + k_{m1} \varphi_{m1} \text{diag}(|e_m|^{\varphi_{m1}-1}) \dot{e}_m + k_{m2} \varphi_{m2} \text{diag}(|e_m|^{\varphi_{m2}-1}) \dot{e}_m) + s_m^T C_m s_m \\ & + s_s^T M_s (\ddot{e}_s + k_{s1} \varphi_{s1} \text{diag}(|e_s|^{\varphi_{s1}-1}) \dot{e}_s + k_{s2} \varphi_{s2} \text{diag}(|e_s|^{\varphi_{s2}-1}) \dot{e}_s) + s_s^T C_s s_s \end{aligned} \tag{36}$$

Since the TVDs $T_1(t)$, $T_2(t)$ and their derivatives are usually bounded [32, 33], then according to (32) and (26) we can get

$$\begin{aligned} \dot{V}_2 = & s_m^T (\tau_m + F_h - C_m \dot{q}_m - g_m + M_m (-\ddot{\hat{q}}_s (t - T_2(t)) (1 - \dot{T}_2(t))^2 \\ & + \dot{\hat{q}}_s (t - T_2(t)) \ddot{T}_2(t) + k_{m1} \varphi_{m1} \text{diag}(|e_m|^{\varphi_{m1}-1}) \dot{e}_m \\ & + k_{m2} \varphi_{m2} \text{diag}(|e_m|^{\varphi_{m2}-1}) \dot{e}_m) + s_m^T C_m s_m + s_s^T (\tau_s + F_e - C_s \dot{q}_s \\ & - g_s + M_s (-\ddot{\hat{q}}_m (t - T_1(t)) (1 - \dot{T}_1(t))^2 + \dot{\hat{q}}_m (t - T_1(t)) \ddot{T}_1(t) \\ & + k_{s1} \varphi_{s1} \text{diag}(|e_s|^{\varphi_{s1}-1}) \dot{e}_s + k_{s2} \varphi_{s2} \text{diag}(|e_s|^{\varphi_{s2}-1}) \dot{e}_s) + s_s^T C_s s_s \end{aligned} \tag{37}$$

Substituting (29)-(31) into (37), we have

$$\begin{aligned} \dot{V}_2 = & -s_m^T k_{m3} M_m \text{sgn}(s_m) - s_m^T k_{m4} M_m \text{sig}(s_m)^{\sigma_{m1}} - s_m^T k_{m5} M_m \text{sig}(s_m)^{\sigma_{m2}} \\ & - s_s^T k_{s3} M_s \text{sgn}(s_s) - s_s^T k_{s4} M_s \text{sig}(s_s)^{\sigma_{s1}} - s_s^T k_{s5} M_s \text{sig}(s_s)^{\sigma_{s2}} \\ \leq & -k_{m4} \|s_m\|^{\sigma_{m1}+1} - k_{m5} \|s_m\|^{\sigma_{m2}+1} - k_{s4} \|s_s\|^{\sigma_{s1}+1} - k_{s5} \|s_s\|^{\sigma_{s2}+1} \\ \leq & -k_{m4} 2^{\frac{\sigma_{m1}+1}{2}} \left\| \frac{1}{2} s_m^2 \right\|^{\frac{\sigma_{m1}+1}{2}} - k_{m5} 2^{\frac{\sigma_{m2}+1}{2}} \left\| \frac{1}{2} s_m^2 \right\|^{\frac{\sigma_{m2}+1}{2}} \\ & - k_{s4} 2^{\frac{\sigma_{s1}+1}{2}} \left\| \frac{1}{2} s_s^2 \right\|^{\frac{\sigma_{s1}+1}{2}} - k_{s5} 2^{\frac{\sigma_{s2}+1}{2}} \left\| \frac{1}{2} s_s^2 \right\|^{\frac{\sigma_{s2}+1}{2}} \\ \leq & -k_4 V_2^{\sigma_1} - k_5 V_2^{\sigma_2} \\ \leq & 0 \end{aligned} \tag{38}$$

where $k_4 = \min(k_{m4}, k_{s4})$, $k_5 = \min(k_{m5}, k_{s5})$, $\sigma_1 = \min(\frac{\sigma_{m1}+1}{2}, \frac{\sigma_{s1}+1}{2})$, $\sigma_2 = \min(\frac{\sigma_{m2}+1}{2}, \frac{\sigma_{s2}+1}{2})$. According to Lemma 1 and (38), the system states converge to the sliding mode surface within a fixed time, and hence the system is stable. Therefore, all signals in $V_2(t)$ are bounded and the reaching time T_{rt} of the system to the sliding surface is bounded by T_{sup1} , that is,

$$T_{rt} \leq T_{sup1} = \frac{1}{k_4} \frac{1}{(1-\sigma_1)} + \frac{1}{k_5} \frac{1}{(\sigma_2-1)} \tag{39}$$

Thus, when the system reaches the sliding mode, we have $s_m = s_s = 0$. Then (27) can be rewritten as

$$\begin{aligned} \dot{e}_m = & -k_{m1} \text{sig}(e_m)^{\varphi_{m1}} - k_{m2} \text{sig}(e_m)^{\varphi_{m2}} \\ \dot{e}_s = & -k_{s1} \text{sig}(e_s)^{\varphi_{s1}} - k_{s2} \text{sig}(e_s)^{\varphi_{s2}} \end{aligned} \tag{40}$$

From Lemma 1 and (40), it can be seen that the position tracking error can converge to zero within a fixed time T_{st} which is bounded by T_{sup2} as follows

$$T_{st} \leq T_{sup2} = \frac{1}{k_1} \frac{1}{(1-\varphi_1)} + \frac{1}{k_2} \frac{1}{(\varphi_2-1)} \tag{41}$$

where $k_1 = \min(k_{m1}, k_{s1}), k_2 = \min(k_{m2}, k_{s2}), \varphi_1 = \min(\varphi_{m1}, \varphi_{s1})$, and $\varphi_2 = \min(\varphi_{m2}, \varphi_{s2})$. From (39) and (41), the convergence time T_{rt} and T_{st} does not depend on the initial states.

Next, the force tracking performance will be proved. Since we have proved that the system is stable, it is clear that $q_i(t) \in \mathcal{L}_\infty, \hat{q}_m(t - T_2(t)) \in \mathcal{L}_\infty$. Then we have $e_s(t - T_2(t)) \in \mathcal{L}_\infty$. As $q_m(t) - \tilde{q}_s(t) = e_s(t - T_2(t)) + \int_0^{T_2(t)} \dot{q}_s(t - \theta)d\theta + q_m - q_s$ and $\int_0^{T_2(t)} \dot{q}_s(t - \theta)d\theta \in \mathcal{L}_\infty$, it can be obtained that $q_m(t) - \tilde{q}_s(t) \in \mathcal{L}_\infty$. Similarly, $q_s(t) - \tilde{q}_m(t) \in \mathcal{L}_\infty$. According to (1), Property 1, Property 3, and Property 4, we have $\ddot{q}_m \in \mathcal{L}_\infty, \ddot{q}_s \in \mathcal{L}_\infty$. Thus, \dot{q}_m and \dot{q}_s are uniformly continuous. According to Barbalat's Lemma [16], it can be deduced that

$$\lim_{t \rightarrow \infty} \dot{q}_i(t) = 0 \tag{42}$$

Further, according to $\ddot{q}_m \in \mathcal{L}_\infty, \ddot{q}_s \in \mathcal{L}_\infty$, using Barbalat's Lemma, one can deduce that $\lim_{t \rightarrow \infty} \ddot{q}_m(t) = 0$ and $\lim_{t \rightarrow \infty} \ddot{q}_s(t) = 0$. According to Theorem 1, we can obtain

$$\lim_{t \rightarrow \infty} (F_h - w_h) = 0, \lim_{t \rightarrow \infty} (F_e - w_e) = 0 \tag{43}$$

From (39) and (41), we have

$$\|s_i\| = 0, \lim_{t \rightarrow \infty} e_i \rightarrow 0, \lim_{t \rightarrow \infty} \dot{e}_i \rightarrow 0 \tag{44}$$

Substituting (42)-(44) into (32), we can get

$$M_m(q_m) \ddot{q}_m = -\wp |w_h - \tilde{w}_e| \tag{45}$$

Multiplying $M_m(q_m)^{-1}$ on both sides of (45) yields

$$\ddot{q}_m = -M_m(q_m)^{-1} \wp |w_h - \tilde{w}_e| \tag{46}$$

From Property 1, it follows that $\frac{1}{\lambda_m} I \leq M_m(q_m)^{-1}$, that is, $-\frac{1}{\lambda} I \wp |w_h - \tilde{w}_e| \geq -M_m(q_m)^{-1} \wp |w_h - \tilde{w}_e|$. Thus,

$$\ddot{q}_m \leq -\frac{1}{\lambda_m} I \wp |w_h - \tilde{w}_e| \tag{47}$$

Since $\bar{\lambda}_m$ is a positive constant and \wp is a positive definite matrix, it follows that $-\frac{1}{\lambda_m} I \wp |w_h - \tilde{w}_e| \leq 0$, that is $\ddot{q}_m \leq 0$. When $-\frac{1}{\lambda_m} I \wp |w_h - \tilde{w}_e| < 0$ and $\ddot{q}_m < 0$, $\sum_{i=1}^n \ddot{q}_{mi} < 0$ holds, where \ddot{q}_{mi} is the i th element of \ddot{q}_m . Hence, there always exists some $\ddot{q}_{mi} < 0$ when $t \rightarrow \infty$, which is inconsistent with the previous conclusion $\lim_{t \rightarrow \infty} \ddot{q}_m(t) = 0$. Thus, we can get $\lim_{t \rightarrow \infty} \ddot{q}_m \rightarrow 0$ and then $\lim_{t \rightarrow \infty} \left(-\frac{1}{\lambda_m} I \wp |w_h - \tilde{w}_e|\right) \rightarrow 0$, that is, $\lim_{t \rightarrow \infty} (|w_h - \tilde{w}_e|) \rightarrow 0$. Therefore, the force tracking error can converge to zero.

4. Experiments

In the teleoperation experimental platform shown in Figure 3, two PHANTOM Omni haptic devices are used. The master is on the left and the slave is on the right. The master is connected to the computer and the slave is connected to the master via IEEE 1394 firewire. Besides, the proposed strategy is implemented in Visual Studio with C++. The haptic device application programming interface of PHANTOM Omni haptic device is called through static linking.

To validate the effectiveness of the proposed strategy, comparative experiments with the scheme in ref. [24] are conducted. In the experiments, the initial positions for the master and slave are $q_m(0) =$

Table 1. Control parameters.

Parameter	Value	Parameter	Value
χ_m	10	$\varphi_{m1}, \varphi_{m2}$	0.1, 1.6
χ_s	10	$\varphi_{s1}, \varphi_{s2}$	0.1, 1.6
$\delta_{1 \min} \sim \delta_{5 \min}$	0.3	δ	diag(60,60)
$\delta_{1 \max} \sim \delta_{5 \max}$	1	σ_{m1}, σ_{m2}	0.8, 3
a	0.5	σ_{s1}, σ_{s2}	0.8, 3
b	-0.1	\mathcal{P}_m	diag(100,6)
$k_{m1} \sim k_{m5}$	0.1, 30, 5, 50, 5	\mathcal{P}_s	diag(1, 1)
$k_{s1} \sim k_{s5}$	0.1, 40, 2, 60, 1	\mathcal{Q}	diag(10, 10)

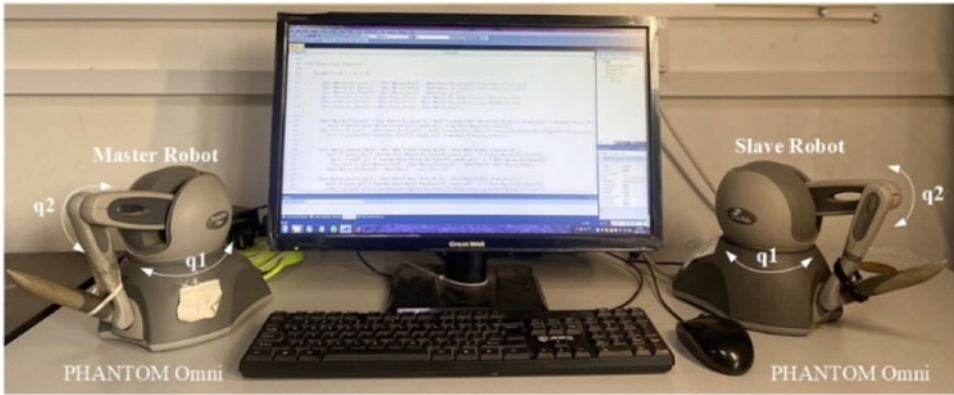


Figure 3. Experimental platform.

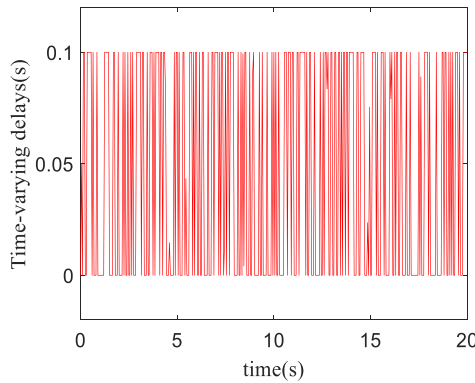


Figure 4. TVDs.

$[q_{m1}(0), q_{m2}(0)]^T = [0.2356, -0.0314]^T$, $q_s(0) = [q_{s1}(0), q_{s2}(0)]^T = [0.1587, 0.0518]^T$, where $q_{i1}(0)$ and $q_{i2}(0)$ $i = \{m, s\}$ represent the initial positions of joints 1 and joint 2. $T_1(t)$ and $T_2(t)$ are shown in Figure 4. The rest of the control parameters are shown in Table 1.

Figure 5 and Figure 6 show the position tracking for the scheme in ref. [24] and the proposed strategy, respectively. As shown in Figure 5, when there are TVDs, the scheme in ref. [24] exhibits significant chattering at the beginning of the experiment. Moreover, when the operator force is applied during 5s–15s, the master and slave fail to achieve satisfactory tracking, resulting in a large position tracking error. In contrast, Figure 6 illustrates that the proposed strategy exhibits no significant chattering in

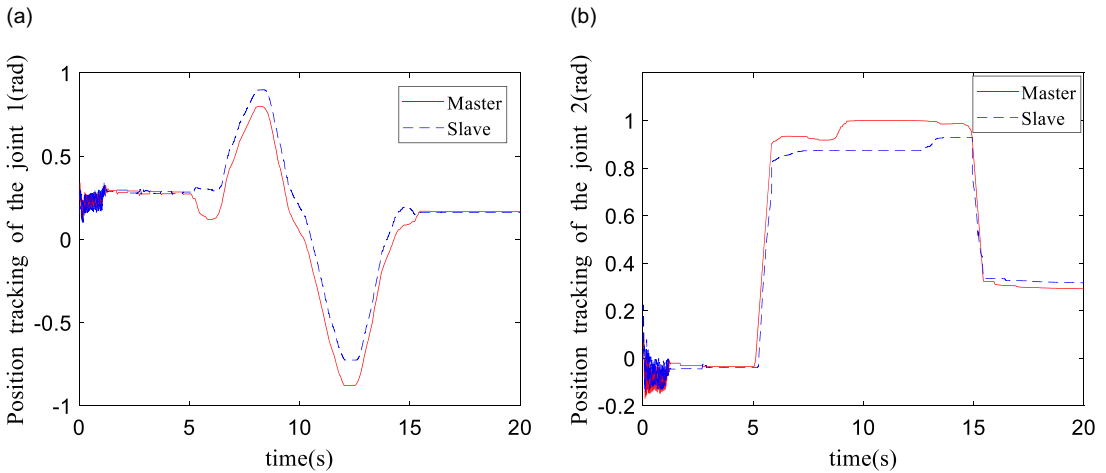


Figure 5. Position tracking (in [24]) (a) Joint 1 (b) Joint 2.

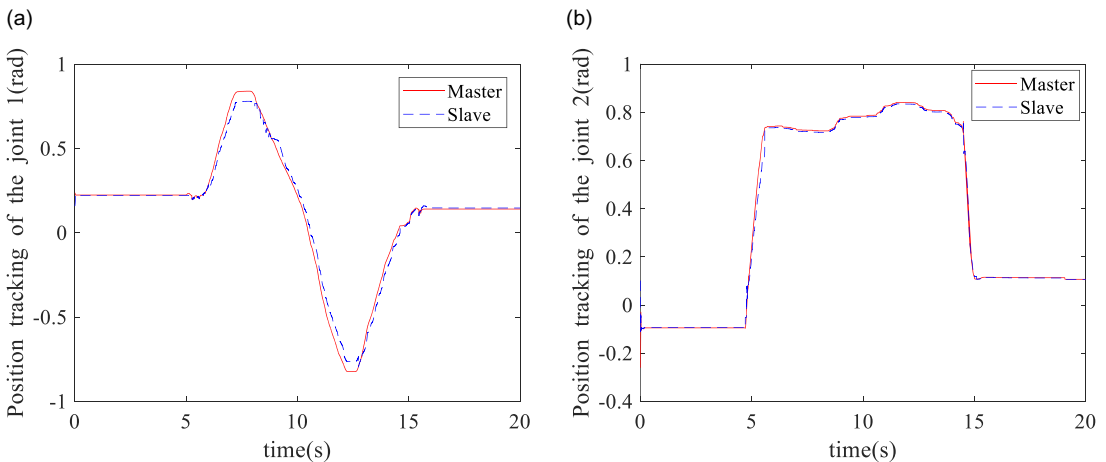


Figure 6. Position tracking (proposed strategy) (a) Joint 1 (b) Joint 2.

position tracking. Furthermore, during the period when the operator force is applied, the slave can rapidly track the master with small position tracking error. This indicates that the proposed strategy has faster transient response, higher tracking accuracy, and minor chattering.

To verify the fixed-time performance, three different initial states are set

$$\text{Case1: } [q_{m_1}(0) \ q_{m_2}(0) \ q_{s_1}(0) \ q_{s_2}(0)] = [-0.1176 \ -0.1239 \ 0.0551 \ 0.2119],$$

$$\text{Case2: } [q_{m_1}(0) \ q_{m_2}(0) \ q_{s_1}(0) \ q_{s_2}(0)] = [0.2056 \ -0.1744 \ -0.1916 \ 0.1883],$$

$$\text{Case3: } [q_{m_1}(0) \ q_{m_2}(0) \ q_{s_1}(0) \ q_{s_2}(0)] = [0.0053 \ -0.1724 \ -0.0740 \ 0.1064]$$

By using (39) and (41), the upper bound of the convergence time for the position tracking error can be obtained as: $T_{\text{sup}} = T_{rt} + T_{st} = \frac{1}{1} \frac{1}{(1-0.8)} + \frac{1}{100} \frac{1}{(2.3-1)} + \frac{1}{5} \frac{1}{(1-0.2)} + \frac{1}{5} \frac{1}{(1.5-1)} = 5.658\text{s}$.

The position tracking for the master and slave under three initial states is shown in Figure 7. It can be observed that the proposed strategy enables the slave and master to achieve tracking within 0.5 s. This implies that the position tracking error converges within the fixed time of 5.658 s as $0.5 \text{ s} \ll 5.658 \text{ s}$. Furthermore, the convergence time does not depend on the initial states.

Figure 8 and Figure 9 show the triggering intervals for the scheme in ref. [24] and the proposed strategy, respectively. From Figure 8, it can be observed that since the fixed triggering thresholds are not related to the system states in ref. [24], the triggering intervals are either very dense or sparse.

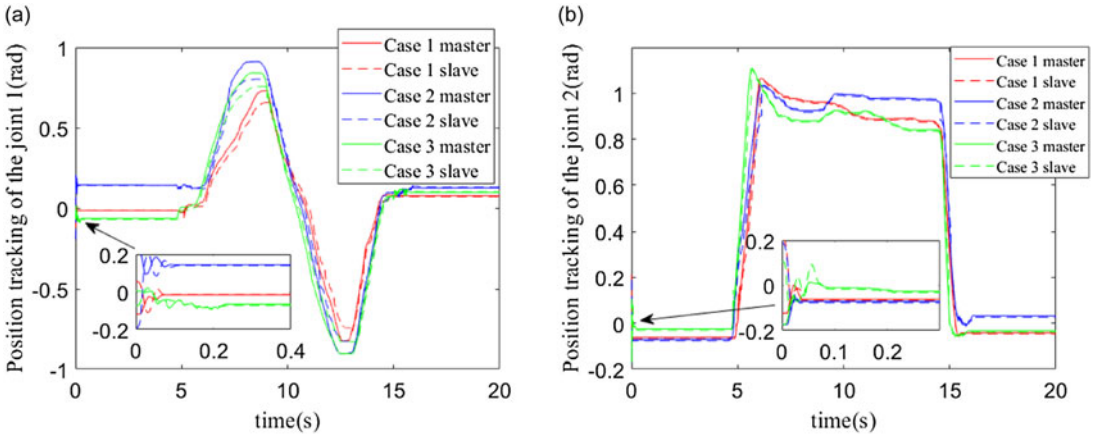


Figure 7. Position tracking under different initial states (a) Joint 1 (b) Joint 2.

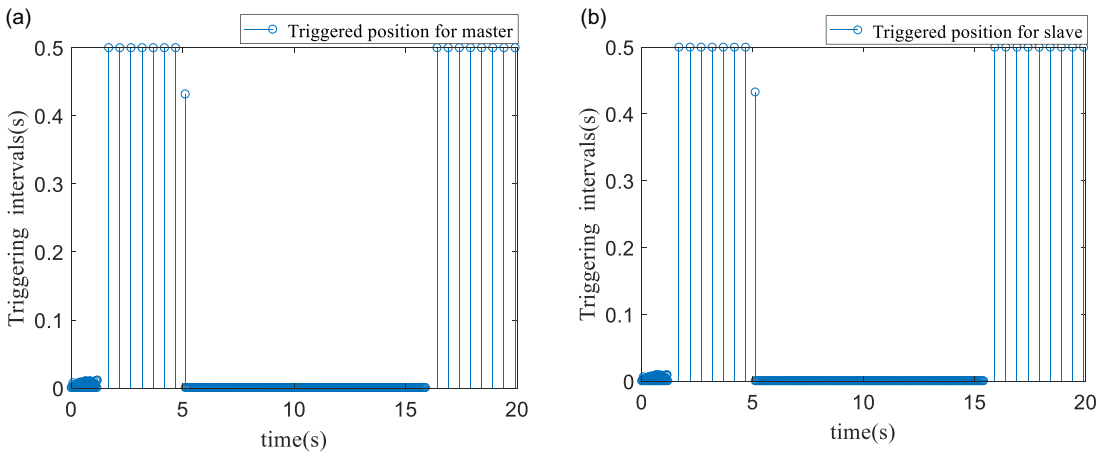


Figure 8. Triggering intervals (in [24]) (a) Master (b) Slave.

In contrast, in Figure 9 the triggering intervals for the proposed strategy are less frequent overall and much sparser. Moreover, since the adaptive triggering thresholds are related to the system states in the proposed strategy, when the operator force is applied during 5 s–15 s, the triggering intervals exhibit considerable variability, demonstrating the flexibility of the proposed strategy.

The experimental results for force tracking of the proposed strategy are illustrated in Figure 10. It can be observed that there is a good tracking performance between the estimate of the operator force and environment force, demonstrating the effectiveness of the FEs in the proposed strategy.

Remark 2. To avoid force measurement in the experiments, the operator force and environment force are estimated by the FEs. Furthermore, from Theorem 1 the estimate errors of the FEs can asymptotically approach zero. Therefore, the estimated forces rather than the measured forces are displayed in Figure 10.

Table 2 compares the average values of the position tracking errors of joint 1 and joint 2, that is, $avg(q_{m1} - q_{s1})$, $avg(q_{m2} - q_{s2})$, and the ratios of the triggering intervals for the master and slave, that is, $RTI_m = (\text{Triggered position data for the master} / \text{Total data}) * 100\%$, $RTI_s = (\text{Triggered position data for the slave} / \text{Total data}) * 100\%$. It can be seen that the proposed strategy has smaller position tracking errors and lower triggering intervals compared to [24].

Table 2. Qualitative comparison of different control methods.

Index	Ref. [24]	Proposed
$avg(q_{m_1} - q_{s_1})(rad)$	0.071765	0.025888
$avg(q_{m_2} - q_{s_2})(rad)$	0.060670	0.006497
RTI_m	57.06%	30.43%
RTI_s	55.13%	25.94%

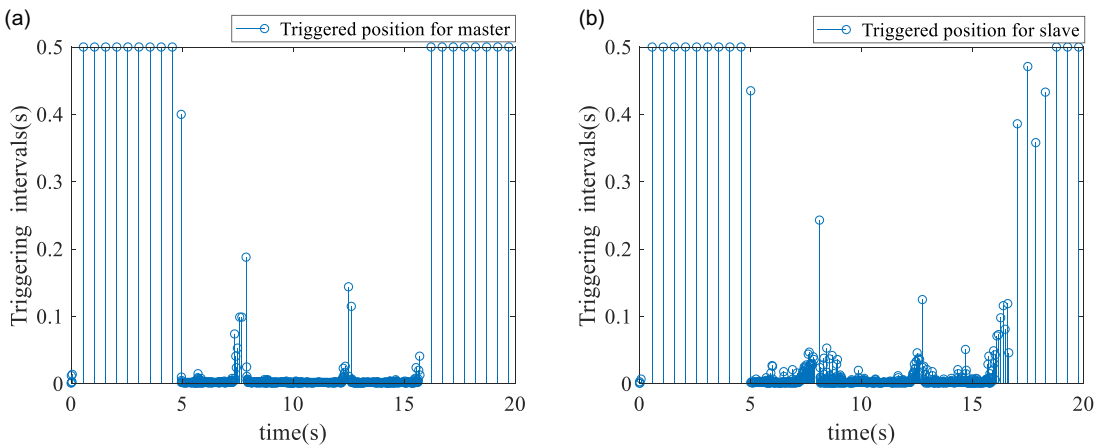


Figure 9. Triggering intervals (proposed strategy) (a) Master (b) Slave.

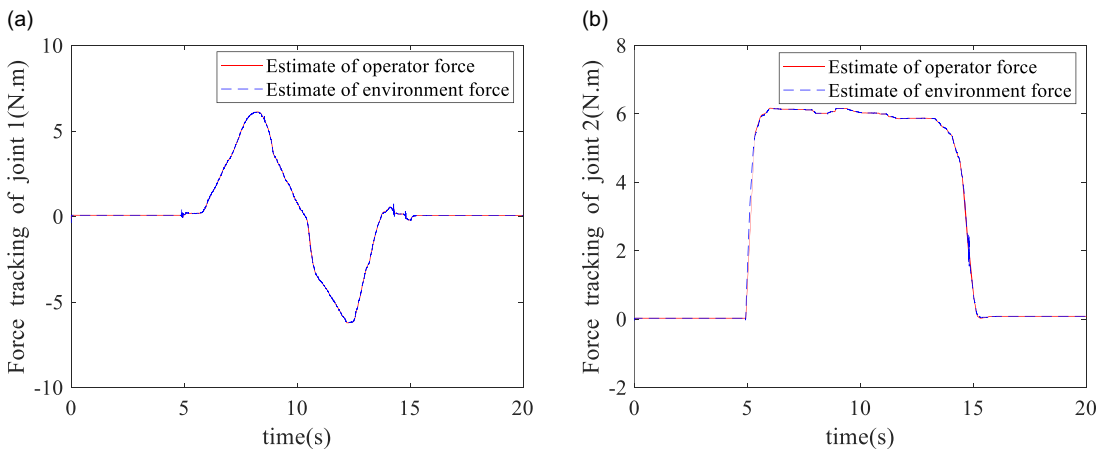


Figure 10. Force tracking (proposed strategy) (a) Joint 1 (b) Joint 2.

5. Conclusions

For a class of teleoperation systems with TVDs and limited bandwidth, this paper proposes a fixed-time control strategy based on adaptive event-triggered communication and FEs. The FEs accurately estimate the operator force and environment force without force sensors. The AETS which correlates the triggering frequency with the system states can save network resources. The SMC achieves fixed-time convergence of the tracking error and the convergence time is independent of the initial conditions. However, in complex communication networks there are other important issues such as cyber-attacks. Therefore, how to extend the proposed strategy to address these issues will remain as our future work.

Author contribution. Xia Liu: Investigation (lead), Methodology (equal), Writing – review and editing (lead), Supervision (lead); Hui Wen: Software (equal), Data curation(lead), Validation(lead), Writing – original draft (lead).

Financial support. This work is supported by Natural Science Foundation of Sichuan Province (No. 2023NSFSC0510) and National Natural Science Foundation of China (No. 61973257).

Competing interests. The authors declare that they have no known competing financial interests or personal relationships that could have appeared to influence the work reported in this paper.

Ethical approval. None.

References

- [1] Y. C. Liu, P. N. Dao and K. Y. Zhao, “On robust control of nonlinear teleoperators under dynamic uncertainties with variable time delays and without relative velocity,” *IEEE Trans Ind Inform* **16**(2), 1272–1280 (2020).
- [2] Y. Yang, X. Feng, J. Li and C. Hua, “Robust fixed-time cooperative control strategy design for nonlinear multiple-master/multiple-slave teleoperation system,” *J Frankl Inst* **360**(3), 2193–2214 (2023).
- [3] P. M. Kebria, A. Khosravi, S. Nahavandi, P. Shi and R. Alizadehsani, “Robust adaptive control scheme for teleoperation systems with delay and uncertainties,” *IEEE Trans Cybernet* **50**(7), 3243–3253 (2020).
- [4] M.-D. Tran and H.-J. Kang, “Adaptive terminal sliding mode control of uncertain robotic manipulators based on local approximation of a dynamic system,” *Neurocomputing* **228**, 231–240 (2017).
- [5] Z. Wang, Z. Chen, B. Liang and B. Zhang, “A novel adaptive finite time controller for bilateral teleoperation system,” *Acta Astronaut* **144**, 263–270 (2018).
- [6] T.-V. Nguyen and Y.-C. Liu, “Advanced finite-time control for bilateral teleoperators with delays and uncertainties,” *IEEE Access* **9**, 141951–141960 (2021).
- [7] Z. Wang, Z. Chen, Y. Zhang, X. Yu, X. Wang and B. Liang, “Adaptive finite-time control for bilateral teleoperation systems with jittering time delays,” *Int J Robust Nonlin Control* **29**(4), 1007–1030 (2019).
- [8] J. Z. Xu, M. F. Ge, T. F. Ding, C. D. Liang and Z. W. Liu, “Neuro-adaptive fixed-time trajectory tracking control for human-in-the-loop teleoperation with mixed communication delays,” *IET Control Theory Appl* **14**(19), 3193–3203 (2021).
- [9] Y. Yang, C. Hua and X. Guan, “Multi-manipulators coordination for bilateral teleoperation system using fixed-time control approach,” *Int J Robust Nonlin Control* **28**(18), 5667–5687 (2018).
- [10] S. Guo, Z. Liu, L. Li, Z. Ma and P. Huang, “Fixed-time personalized variable gain tracking control for teleoperation systems with time varying delays,” *J Frankl Inst* **360**(17), 13015–13032 (2023).
- [11] F. Azimifar, M. Abrishamkar, B. Farzaneh, A. A. D. Sarhan and H. Amini, “Improving teleoperation system performance in the presence of estimated external force,” *Robot Comp Integr Manuf* **46**, 86–93 (2017).
- [12] L. Han, J. Mao, P. Cao, Y. Gan and S. Li, “Toward sensorless interaction force estimation for industrial robots using high-order finite-time observers,” *IEEE Trans Ind Electron* **69**(7), 7275–7284 (2022).
- [13] C. Yang, G. Peng, L. Cheng, J. Na and Z. Li, “Force sensorless admittance control for teleoperation of uncertain robot manipulator using neural networks,” *IEEE Trans Syst Man Cybern Syst* **51**(5), 3282–3292 (2021).
- [14] F. Azimifar, K. Hassani, A. H. Saveh and F. T. Ghomshe, “Performance analysis in delayed nonlinear bilateral teleoperation systems by force estimation algorithm,” *Trans Inst Meas Control* **40**(5), 1637–1644 (2017).
- [15] M. Namnabat, A. H. Zaeri and M. Vahedi, “A passivity-based control strategy for nonlinear bilateral teleoperation employing estimated external forces,” *J Braz Soc Mech Sci Eng* **42**(12), 1–10 (2020).
- [16] S. A. M. Dehghan, H. R. Koofgar, H. Sadeghian and M. Ekramian, “Observer-based adaptive force-position control for nonlinear bilateral teleoperation with time delay,” *Control Eng Pract* **107**, 1–10 (2021).
- [17] Y. Yang, F. Guo, J. Li and X. Luo, “New delay-dependent position/force hybrid controller design for uncertain telerobotics without force sensors,” *Trans Inst Meas Control* **46**(2), 253–267 (2023).
- [18] Y. Yuan, Y. Wang and L. Guo, “Force reflecting control for bilateral teleoperation system under time-varying delays,” *IEEE Trans Ind Inform* **15**(2), 1162–1172 (2019).
- [19] N. Zhao, P. Shi, W. Xing and R. K. Agarwal, “Resilient event-triggered control for networked cascade control systems under denial-of-service attacks and actuator saturation,” *IEEE Syst J* **16**(1), 1114–1122 (2022).
- [20] S. C. Hu, C. Y. Chan and Y. C. Liu, “Event-Triggered Control for Bilateral Teleoperation with Time Delays,” **In: IEEE International Conference on Advanced Intelligent Mechatronics**, Banff, Canada (IEEE, 2016) pp. 1634–1639.
- [21] Y. C. Liu and S. C. Hu, “Nonlinear bilateral teleoperators under event-driven communication with constant time delays,” *Int J Robust Nonlin Control* **29**(11), 3547–3569 (2019).
- [22] C. Li, Y. Li, J. Dong and H. Wang, “Event-triggered control of teleoperation systems with time-varying delays,” **In: China automation congress**, Beijing, China, (2021) pp.1537–1542.
- [23] S. C. Hu and Y. C. Liu, “Event-triggered control for adaptive bilateral teleoperators with communication delays,” *IET Control Theory Appl* **14**(3), 427–437 (2020).
- [24] H. Gao and C. Ma, “Event-triggered aperiodic intermittent sliding-mode control for master-slave bilateral teleoperation robotic systems,” *Indu Robot Int J Robot Res Appl* **50**(3), 467–482 (2023).

- [25] Y. Zhao, P. X. Liu and H. Wang, “Adaptive event-triggered synchronization control for bilateral teleoperation system subjected to fixed-time constraint,” *Int J Adapt Control Signal Process* **36**(8), 2041–2064 (2022).
- [26] Z. Wang, H. K. Lam, B. Xiao, Z. Chen, B. Liang and T. Zhang, “Event-triggered prescribed-time fuzzy control for space teleoperation systems subject to multiple constraints and uncertainties,” *IEEE Trans Fuzzy Syst* **29**(9), 2785–2797 (2021).
- [27] M. V. de Lima, L. A. Mozelli, A. A. Neto and F. O. Souza, “A simple algebraic criterion for stability of bilateral teleoperation systems under time-varying delays,” *Mech Syst Signal Process* **137**, 1–11 (2020).
- [28] X. Yu, W. He, H. Li and J. Sun, “Adaptive fuzzy full-state and output-feedback control for uncertain robots with output constraint,” *IEEE Trans Syst Man Cybern Syst* **51**(11), 6994–7007 (2021).
- [29] R. E. Bavili, A. Akbari and R. M. Esfanjani, “Control of teleoperation systems in the presence of varying transmission delay, non-passive interaction forces, and model uncertainty,” *Robotica* **39**(8), 1451–1467 (2021).
- [30] L. Chan, Q. Huang and P. Wang, “Adaptive-observer-based robust control for a time-delayed teleoperation system with scaled four-channel architecture,” *Robotica* **40**(5), 1385–1405 (2022).
- [31] H. Du, G. Wen, D. Wu, Y. Cheng and J. Lu, “Distributed fixed-time consensus for nonlinear heterogeneous multi-agent systems,” *Automatica* **113**, 1–11 (2020).
- [32] H. Shen and Y. J. Pan, “Improving tracking performance of nonlinear uncertain bilateral teleoperation systems with time-varying delays and disturbances,” *IEEE-ASME Trans Mechatron* **25**(3), 1171–1181 (2020).
- [33] H. Zhang, A. Song, H. Li, D. Chen and L. Fan, “Adaptive finite-time control scheme for teleoperation with time-varying delay and uncertainties,” *IEEE Trans Syst Man Cybern Syst* **52**(3), 1552–1566 (2022).

Cite this article: X. Liu and H. Wen, “Fixed-time control of teleoperation systems based on adaptive event-triggered communication and force estimators”, *Robotica*. <https://doi.org/10.1017/S0263574724001310>